Available online at www.sciencedirect.com
SCIENCE DIRECT®

Journal of the European Ceramic Society 24 (2004) 33–44

www.elsevier.com/locate/jeurceramsoc

Microstructural and microtextural investigations of boron nitride deposited from BCl_3–NH_3–H_2 gas mixtures

S. Le Gallet[a], G. Chollon[a,*], F. Rebillat[a], A. Guette[a], X. Bourrat[a], R. Naslain[a], M. Couzi[b], J.L. Bruneel[b]

[a]*Laboratoire des Composites Thermostructuraux, UMR-5801 (CNRS-Snecma-CEA-UB1), 3 allée de la Boétie, Domaine Universitaire, 33600 Pessac, France*
[b]*Laboratoire de Physico-Chimie Moléculaire, UMR-5803, 351, cours de la Libération, 33405 Talence, France*

Received 6 October 2002; received in revised form 3 March 2003; accepted 7 March 2003

Abstract

The structural, morphological and textural characteristics of BN coatings processed by CVD from (BCl_3, NH_3, H_2) gas mixtures, at low pressure ($P = 1.3$ kPa) and low temperature ($T = 800$ °C), with different Q_{NH3}/Q_{BCl3} gas flow rate ratios, have been investigated. Whereas the as-processed coatings are amorphous, a high degree of crystallisation can be achieved after a post-deposition heat treatment. The sole post-elaboration heat treatment does not allow the improvement of the crystallisation degree of the boron nitride. The presence of a small amount of oxygen, resulting from a simple exposure of the coating to a controlled atmosphere (temperature, moisture rate), is also necessary. For given temperature and pressure, a wide range of microstructures of the heat-treated BN coatings, from isotropic to anisotropic, can be observed by varying the Q_{NH3}/Q_{BCl3} ratio.

Keywords: BN; Coatings; Composites; Grain growth; Microstructure-final

1. Introduction

The development of BN coatings for aeronautic engine applications has been motivated by the will of improving the mechanical properties and the lifetime of non-oxide ceramic matrix composites (CMCs). Boron nitride as an interphase material (e.g. in SiC/SiC composites) is indeed an interesting alternative to pyrocarbon that is generally used. Carbon and boron nitride both display hexagonal crystallographic structures with a low interplanar bond energy (17 kJ/mol for hexagonal BN[1] and 7 kJ/mol for graphite) and a high intraplanar bond energy (636 kJ/mol for hexagonal BN[2] and 524 kJ/mol for graphite). In standard CVD conditions, the most organised forms of boron nitride and carbon are only turbostratic, i.e., they show stacking faults of the (002) planes. The (002) planes are generally observed to be parallel to the surface of the fibres, an orientation promoting the deflection of the matrix cracks from mode I to mode II in the fibre/matrix (FM) interfacial zone.[3]

The main advantages of boron nitride as an interphase in SiC/SiC composites with regard to carbon are (i) its better oxidation resistance (the temperature onset of oxidation is 800 °C versus 450 °C for carbon) and (ii) the formation of B_2O_3 in a condensed form (owing to its low volatilisation pressure in dry air up to about 950 °C) during oxidation.[4,5] However, the oxidation resistance of the boron nitride coatings depends on their crystallisation degree.[5]

The BN coatings are commonly processed by chemical vapour deposition (CVD) or infiltration (CVI) from various gas precursors. The (BCl_3, NH_3, H_2) gas mixtures give rise to high coating rates at temperatures as low as 800 °C. The (BF_3, NH_3, Ar) gas system leads to a boron nitride better organised than that obtained from the (BCl_3, NH_3, H_2) system. However, BF_3 and HF (the latter resulting from the reaction of BF_3 with NH_3) being very aggressive with regard to the SiC fibres, the (BF_3, NH_3, Ar) gas system is not much used.[6,7]

* Corresponding author. Tel.: +33-5-56-84-47-27; fax +33-5-56-84-12-25.
E-mail address: chollon@lcts.u-bordeaux.fr (G. Chollon).

0955-2219/03/$ - see front matter © 2003 Elsevier Ltd. All rights reserved.
doi:10.1016/S0955-2219(03)00126-2

By covering large domains of α ratio ($\alpha = Q_{NH3}/Q_{BF3}$, where Q_i is the gas flow rate specie i) T and P conditions, Jacques et al. and Rebillat et al.[8,9] have obtained BN coatings from the (BF_3, NH_3, Ar) system, with microtextures ranging from isotropic to anisotropic. In the same way, a significant effect of the processing parameters upon the microtexture of the coatings can be expected for the (BCl_3, NH_3, H_2) system.

Boron nitride coatings, processed from the (BCl_3, NH_3, H_2) gas system in standard CVD/CVI conditions (i.e. low temperature and pressure), are not stable in air at room temperature.[10–13] This instability results from an absorption of oxygen-bearing species such as O_2 and/or H_2O. Some authors have therefore carried out post-deposition heat treatments at high temperatures (ranging from 1000 to 1700 °C[5,12,14]) to reduce the reactivity of the boron nitride deposits with oxygen. This effect is obtained by achieving the decomposition of the unreacted species and by increasing the crystallisation degree of the coating. However, Lacrambe[12] established that the ability of boron nitride to crystallise during a post-deposition heat treatment depends on the initial presence of oxygen in the coating. The influence of oxygen on the crystallisation of boron nitride had already been investigated by Thomas et al.[15] These authors have indeed showed that a turbostratic BN powder (BN_t) was transformed into the hexagonal BN phase (BN_h) at a temperature as low as 1450 °C, by adding a B_2O_3 powder, whereas the $BN_t \rightarrow BN_h$ transformation in the absence of B_2O_3 generally occurs beyond 2000 °C.

The present paper deals with the influence of the processing conditions on the microstructure/texture of CVD-BN coatings, by means of various and complementary techniques. Besides the typical CVD parameters ($\alpha = Q_{NH3}/Q_{BCl3}$, T), the effect of a post-deposition heat treatment associated with a careful monitoring of the oxygen amount in the coating has been particularly examined.

2. Experimental procedure

2.1. CVD processing conditions and materials studied

The boron nitride coatings were deposited in a hot-wall low-pressure chemical vapour deposition (CVD) reactor from the (BCl_3, NH_3, H_2) gas system. Because of the high reactivity of BCl_3, the temperature and the pressure were chosen relatively low and maintained constant. The inlet composition of the gas phase is defined from the gas flow rates (Q_i), by the two parameters $\alpha = Q_{NH3}/Q_{BCl3}$ and $\beta = Q_{H2}/(Q_{BCl3} + Q_{NH3})$. Q_{BCl3} and Q_{H2} were maintained constant whereas Q_{NH3} and therefore α, was varied (with $1 \leqslant \alpha_1 < \alpha_2 < \alpha_3$). The coatings were deposited on sintered α-SiC substrates or SiC-based fibres (Hi-Nicalon from Nippon Carbon). The thickness of the coatings deposited with α_1, α_2 and α_3 ratios was respectively 2–4, 7–8 and 10–16 μm. The various processing conditions investigated are summed up in the Table 1. The as-processed coatings were further submitted to heat treatments in pure argon at a temperature T ranging from 1000 to 1300 °C. The as-processed CVD-coatings were temporarily exposed to ambient air at room temperature before the heat treatment (see Section 3.2.1).

Structures of the studied coatings were compared with those of commercial boron nitrides supplied by Advanced Ceramics and Aldrich. The boron nitride sample from Advanced Ceramics (referred to as AC–BN) is a bulk material processed by CVD also from the (BCl_3, NH_3, H_2) gas system but at a temperature of about 2000 °C. The boron nitride from Aldrich (noted A-BN) is a crystalline powder prepared from boron oxide and ammonia.

2.2. Structural and chemical characterisation

The microstructure of the BN coatings was characterised by X-ray diffraction (XRD) with a $\theta/2\theta$ diffractometer (Siemens D5000, $\lambda_{CuK_{\alpha 1}} = 0.15405$ nm). A small amount of silicon powder was used to correct the position of the diffraction peaks. The dimensions of the coherent domains, La and Lc, were calculated from the Scherrer's equation $L = k\lambda/\Gamma\cos\theta$, where the k constant is taken equal to 1.54 or 0.9 (respectively for the hkl or $00l$ line), Γ is full width at half height (in radian), λ the wavelength of the Cu-$K_{\alpha 1}$ line and θ the diffraction angle.

The pole figures corresponding to ($00l$) planes were recorded from coatings deposited on a flat substrate to show the distribution of the orientation of the ($00l$) planes with respect to the substrate. The X-ray source and detector were set horizontally in the ($00l$) Bragg conditions and the intensity of the diffracted beam was recorded versus the horizontal tilt angle χ (ranging from 0 to 90°). The anisotropy degree of the coating is directly related to the decreasing rate of diffracted intensity when χ increases from 0° (i.e., of the sharpness of the pole figure).

The Raman microspectrometry (RMS) analyses (Labram 10 spectrometer from Jobin Yvon) were carried out from the surface of the boron nitride coatings, without any specific preparation of the sample. The monochromatic exciting source was the 514.5 nm line of an Ar^+ laser. The analyses were performed in the punctual mode and the lateral resolution of the laser spot was of the order of 1–2 μm with a 100× objective. The power of the

Table 1
Processing conditions of the BN coatings at $T = 800$ °C and $P = 1.3$kPa

	α	β	Coating rate (μm/h)
BN(α_1)	$\alpha_1 \geqslant 1$	0.5	1.8
BN(α_2)	$\alpha_2 = \alpha_1 + 0.3$	0.4	6
BN(α_3)	$\alpha_3 = \alpha_1 + 0.6$	0.4	10

incident laser was maintained below 0.5 mW to avoid any local heating of the sample. The fluorescence of some of the samples made difficult the RMS analyses. This phenomenon of fluorescence, which is only observed for the CVD-BN coatings, would be explained by the presence of impurities such as oxygen and carbon.[16] Hexagonal BN is characterised by two Raman active modes, with an E_{2g} symmetry. These two modes are due to in-plane atomic vibrations. Whereas the first one (E_{2g1}) involves a shear displacement between successive planes, the second one (E_{2g2}) corresponds to the elongation vibration of intra-layer B–N bonds.[16]

Transmission electron microscopy (TEM) measurements were performed with a Philips CM30ST microscope, having a resolution of 0.2 nm. The analyses were carried out according to conventional procedures, i.e., the (002)-dark field, selected area electron diffraction (SAD) and (002)-lattice fringe high-resolution modes, to compare the microtexture/structure of the coatings at different stages of their processing. The misalignment of the boron nitride layers with respect to the anisotropy plane affects the shape of the 002 reflections on the SAD pattern to form arcs instead of the two opposite spots ideally observed for a single crystal.

The electron energy loss spectroscopy (EELS) was used to evidence and quantify the elements present in the sample (Gatan, PEELS 666). The atomic concentration ratios were calculated from the energy peak areas (for example, 188 eV for B and 401 eV for N) on the EELS spectra and compared for the various boron nitride coatings.

The as-processed coatings, because of their high sensibility to air were deposited as thin films (<0.25 μm) on carbon grids and were observed without any further preparation, to avoid any structural modification of the sample.

The heat-treated samples, because of their higher chemical stability, were prepared following usual techniques (epoxy mount, mechanical thinning, polishing and ion-milling with a Gatan Duo-mill).

Auger electron spectroscopy (AES) analyses were performed with a scanning microprobe (VG Microlab 310-F) equipped with a field emission gun and an Ar^+ ion-sputtering gun for depth profiling. The intensities (peak area mode) of the Auger electron peaks (B-KLL, C-KLL, N-KLL, O-KLL transitions) were plotted as a function of the sputtering time (sputtering rate: 0.3 nm/min with Ta_2O_5 as reference).

3. Results and discussion

3.1. CVD coating rates

The significant and regular increase of the coating rate with the α ratio suggests that the yield of the reaction is not optimum in the case of the α_1 and α_2 values (Table 1). The BN yield calculated from the thermodynamic data should be nevertheless expected to be maximum for a ratio $\alpha = Q_{NH3}/Q_{BCl3}$ equal to 1. However, despite the NH_3 excess ($\alpha > 1$), the formation of ammonium chloride in the gaseous phase strongly reduces the NH_3 concentration, limiting the reaction with BCl_3 and therefore the formation of boron nitride.

3.2. Influence of the post-deposition heat treatments

3.2.1. Role of oxygen on the crystallisation of boron nitride

The furnaces used for the CVD processing and the heat treatment of the coatings being different, the as-processed BN coatings were temporarily exposed to air before the post-deposition heat treatment. The high reactivity of the as-processed BN (poorly crystallised and still containing some unreacted species) makes the absorption of oxygen inevitable. The amount of oxygen absorbed by the BN coating (as measured by AES) can reach a concentration as high as about 8 at.% after 1 day of exposure to ambient air at room temperature. To better show the role of oxygen in the ability of the boron nitride to crystallise at a relatively low temperature ($\leqslant 1300$ °C), the XRD spectra of BN coatings obtained according to various processing conditions have been compared (Fig. 1). The three spectra shown in Fig. 1 respectively correspond to (i) an as-processed BN coating, (ii) a BN coating covered with a CVD SiC layer deposited in the same furnace as that used for the BN and subsequently heat treated (i.e., without any exposure to air of the BN) and (iii) a BN coating previously exposed to air before being covered with a SiC layer and heat treated.

Whereas the third BN coating contains oxygen, AES analyses have shown that the second one, not exposed to air, is oxygen-free. The comparison of the three spectra shows that the crystallisation degree of the oxygen-free coating is unchanged after heat treatment,

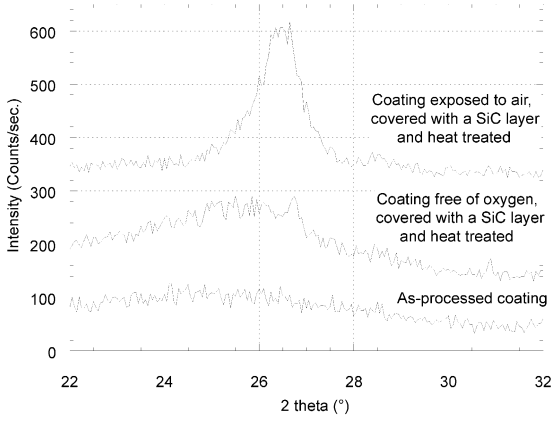

Fig. 1. Effect of oxygen on the crystallisation of the BN coatings.

whereas the boron nitride containing oxygen has obviously crystallised to some extent.

These features clearly show that the presence of oxygen is essential to achieve the crystallisation of the boron nitride coatings at a relatively low temperature ($\leqslant$1300 °C).

3.2.2. Thermogravimetric analyses

A sample of BN coating, previously exposed to air, was heat treated at a temperature of 1300 °C for 2 h 30 min in pure argon and its mass variation recorded during the heat treatment, by thermogravimetric analysis (TGA, Fig. 2). The mass loss is about 15% after a 2 h 30 min treatment. The main part of the mass loss occurs during the temperature rise and is about 14% of the total mass of the Hi-Nicalon fibres coated with BN, i.e., about 18% of the initial mass of BN. The mass loss observed during the dwell at 1300 °C is low (1%) and almost constant after 20 min. The crystallisation process occurring at 1300 °C is thought to be related to the volatilisation observed by TGA. Previous studies have showed that the crystallisation of boron nitride at high temperature does not significantly depend on the annealing time at a given temperature but rather on the temperature. Choi and Kang[17] have shown that at a temperature allowing the turbostratic→hexagonal BN conversion (T=1350 °C) and in presence of H_3BO_3, the transformation was fully completed after only few minutes. The duration chosen here for the treatment of the BN coatings (2 h 30 min) was therefore supposed to be long enough to achieve the organisation of the coating.

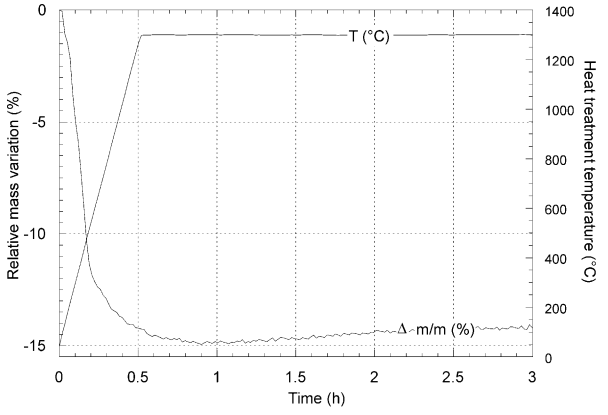

Fig. 2. Thermogravimetric analysis of a heat treated BN coating.

3.2.3. Gas analysis

The mass loss and the crystallisation of the boron nitride at high temperature correspond to the emission of volatile species. To identify the gaseous species formed during the heat treatment of the boron nitride coatings, a gas analysis coupled with the TGA was carried out. The gaseous phase was taken from the hot zone and driven into a mass spectrometer. The ions (molecular and fragments) derived from the molecules of the gaseous phase are discriminated according to their mass and their electronic charge (m/z ratio with z being mainly equal to 1). The intensity of the ion current recorded during the analysis is proportional to the amount of ionised species formed in the spectrometer. The evolution of the ion currents corresponding to the m/z values reported in the Table 2 has been recorded versus time. The attribution of the ion masses to the gaseous species is sometimes difficult, especially for the low m/z values. The release of various gaseous species is detected from the evolution of the ion current, depending on the temperature range and the m/z values. Four main temperature domains are observed at about 225 °C (for the 14, 15, 16, 17, 18, 70, 81 and 83 m/z ratios), 930 °C (m/z=26, 27), 1060 °C (m/z=12, 14, 22, 28, 43, 44, 45, 46, 48) and 1300 °C (m/z=12, 14, 28, 44).

In spite of few uncertainties due to the fact that different compounds may have similar m/z values, the volatilisation of some species can be evidenced from the evolution of the ion currents of the molecular species and their fragments. The lowest temperature domain (about 225 °C) corresponds to the emission of the BN gaseous precursors (NH_3 and BCl_3), probably unreacted and trapped within the coating as well as H_2O, resulting from the exposure of the coating to the air. The second temperature domain (about 930 °C) corresponds to the formation of HCN. BH_3 and H_2BO_2 are emitted within the third temperature domain (T∼1060 °C) and in a lower extent, within the fourth domain (up to 1300 °C).

Table 2
m/z Ratios and gaseous species investigated by mass spectrometry

m/z	Gaseous species	m/z	Gaseous species	m/z	Gaseous species
2	H_2	27	HCN/BO	46	NO_2
12	C/BH	28	N_2/CO/C_2H_4/B_2H_6/HBO	46–48	BCl/CHCl/H_2BCl/C_4/O_3
14	N/BH_3/CH_2	30	N_2H_2/NO/H_2CO	62	H_3BO_3/NO_3/C_2HCl/BOCl
15	NH/CH_3	32	O_2/N_2H_4	70	B_2O_3
16	NH_2/O/CH_4	35–37	Cl	70–74	Cl_2
17	NH_3/OH	36–38	HCl/B_2O/C_2N/C_2	81–85	BCl_2/$B_3N_3H_6$/NO_2Cl
18	H_2O	40	Ar/NCN	116–122	BCl_3
20	Ar	43	BO_2/HNCO	132	$H_3B_3O_6$
26	CN/C_2H_2	44	CO_2/HBO_2/N_2O/C_2H_4O		

The AES analyses showed that the BN coatings do not contain carbon, excepted a slight contamination at the very near surface. The m/z ratios were therefore preferentially attributed to carbon free species. A release of HCN was nevertheless observed, which might arise from a possible interfacial reaction between the carbon of the fibre and the BN coating at high temperature.

The high temperature mass loss associated with the volatilisation of BH_3 and H_2BO_2, which is still observed up to the end of the heat treatment, suggests that the physico-chemical phenomena occurring during the heat treatment be not fully achieved. However the volatilisation is weak after 2 h 30 min at 1300 °C, while no significant improvement of the crystallisation degree is expected at this temperature with a longer treatment.

The crystallisation of the BN coating occurs simultaneously with the volatilisation of gaseous species, bearing respectively boron and nitrogen. The volatilisation of the boron and the nitrogen of the coating are thought to be responsible for the structural reorganisation of the coating via a complex process. The presence of a solid or viscous intergranular phase containing boron and oxygen and partially volatilising at high temperature, might be involved in the crystallisation of the boron nitride through a grain boundary diffusion mechanism.

3.2.4. Characterisation of the heat-treated coatings

The XRD spectra of the as-processed and heat-treated BN coatings are presented in Fig. 3 and in Tables 3 and 4. All spectra show the (002) diffraction peak. The full width at half height of the (002) line is very large before the post-deposition heat treatment, a feature characteristic of a very poorly organised material. The (002) line becomes sharper after the post-deposition heat treatment.

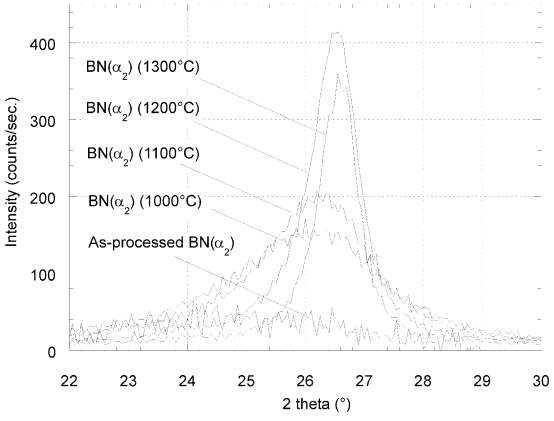

Fig. 3. Influence of the heat treatment temperature on the XRD characteristics.

Table 3
Influence of the α ratio on the XRD characteristics and on the E_{2g2} band features for a BN coating treated at 1300 °C

	XRD characteristics		E_{2g2} band features	
	d_{002} (nm)	Lc (nm)	ν (cm^{-1})	$\Delta\nu$ (cm^{-1})
BN(α_1)	0.339	4.2	1371	28
BN(α_2)	0.338	9.9	1368	20
BN(α_3)	0.337	10.1	1369	20

On the Raman spectra, for a given coating, the heat treatment at an increasing temperature results in a gradual decrease of the frequency at the band maximum ($\nu_{E_{2g2}}$) and of the full width at half maximum ($\Delta\nu_{E_{2g2}}$). There is a linear relationship between $\Delta\nu_{E_{2g2}}$ and $\nu_{E_{2g2}}$ for all tested samples except for the as-processed coatings which significantly deviate from the general trend (Fig. 4). These data are in rather good agreement with those from Nemanich et al.[16] Nemanich et al. have indeed shown that good correlations exist between the average size of the coherent h-BN domains (La) as determined by XRD and the E_{2g2} band features ($\nu_{E_{2g2}}$ and $\Delta\nu_{E_{2g2}}$):

$$\Delta(\mathrm{cm}^{-1}) = 38/La(\mathrm{nm}) - 0.29$$
$$\Delta\nu_{E_{2g2}}(\mathrm{cm}^{-1}) = 141.7/La(\mathrm{nm}) + 8.70$$

where Δ is the frequency shift of the peak from the value corresponding to the largest cristallite sample (1366 cm^{-1} as found in XBN-1).[16]

The evolution of the E_{2g2} band features with the heat treatment temperature is directly related to the

Table 4
Influence of the heat treatment temperature on the XRD characteristics for the BN(α_2) coating

	d_{002} (nm)	Lc (nm)
1000 °C	0.343	2.8
1100 °C	0.342	3.8
1200 °C	0.339	9.1
1300 °C	0.338	11.1

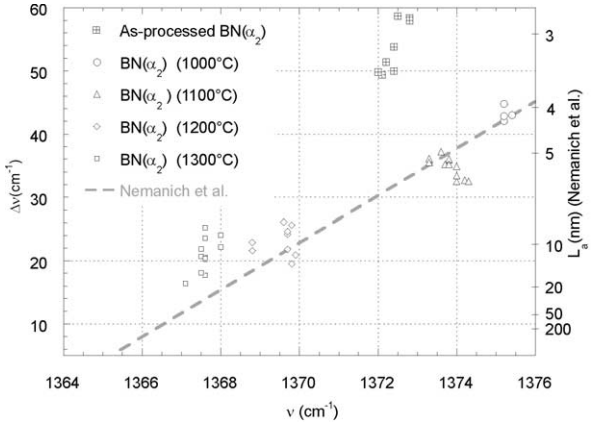

Fig. 4. Influence of the heat treatment temperature on the E_{2g2} band features.

structural organisation of the h-BN phase in the CVD coatings.

In spite of a relatively low temperature ($\leqslant$1300 °C) (with respect to the temperature generally required to crystallise BN), the heat treatment improves significantly the crystallisation degree of the BN coating.

3.3. Influence of the α ratio

3.3.1. Characterisation of the various coatings

The as-processed boron nitride coatings prepared from various conditions [BN(α_1), BN(α_2) and BN(α_3)], because of their poorly organised microstructure, do not show significantly different features in their XRD spectra. Only the heat-treated coatings have been considered to show the influence of the α ratio on the XRD spectra (Table 3). The d_{002} inter-reticular distances of the BN(α_1), BN(α_2) and BN(α_3) coatings are significantly larger than that of the h-BN crystal (0.333 nm). The crystallisation degree of the coatings (as assessed through the *Lc* parameter) increases with the α ratio, particularly between α_1 and α_2. Although the spectra show a relatively sharp (002) line, indicative of a relatively high crystallisation degree, the (100) and (101) lines (or at least the multicomponent (10) band) are not discernible. A preferential orientation of the crystallites flat upon the substrate might explain that the number of (100) and (101) planes being in the Bragg position is too low to lead to diffraction peaks. The pole figure (not shown here) centred on the (002) reticular plane, carried out on the heat-treated BN(α_1), BN(α_2) and BN(α_3) coatings, shows that the (002) planes are oriented preferentially parallel to the surface of the substrate. The largest full width at half maximum (FWHM) of the BN(α_1) pole figure denotes the poorest anisotropy of the three coatings.[18]

The Raman data corresponding to the BN(α_1), BN(α_2) and BN(α_3) coatings are presented in Table 3. The E_{2g2} band characteristic of h-BN appears in all spectra. The frequency ($\nu_{E_{2g2}}$) and the width ($\Delta\nu_{E_{2g2}}$) of the E_{2g2} band are very close for the heat treated BN(α_2) and BN(α_3) coatings while significantly larger for the BN(α_1) coating.

3.3.2. Comparison with commercial BN

The structure of the BN(α_1), BN(α_2) and BN(α_3) coatings were compared with those of the commercial AC–BN and A–BN specimens.

For the AC–BN, two XRD spectra have been recorded, respectively from the surface of the sample (i.e. with the normal direction perpendicular to the (002) planes) and from the edge of the sample (i.e. with the normal direction parallel to the (002) planes) (Fig. 5). The ratios of the intensities between the (002) line and the (10) band are completely different for the two spectra, highlighting the marked anisotropic character of the high temperature CVD–BN coating. The FWHM of the pole figure indeed confirms the high degree of anisotropy of the AC–BN, with a value very close to those of both BN(α_2) and BN(α_3) coatings. Furthermore, the AC-BN shows a (002) line with features close to those of the BN(α_1), BN(α_2) and BN(α_3) coatings but with a well defined (10) band [though the (100) and (101) lines being not fully resolved]. The A–BN is the most crystallised sample of all tested BN materials, with well-separated and sharp lines (Fig. 6).

The MSR analyses correlate rather well with the structural analyses by XRD. Both $\nu_{E_{2g2}}$ and $\Delta\nu_{E_{2g2}}$ values are relatively close for the AC–BN, BN(α_2) and BN(α_3) samples, while significantly higher for the BN(α_1) coating (Fig. 7). From all the tested samples, the A–BN shows the lowest $\nu_{E_{2g2}}$ frequency (1366 cm^{-1}) and half width (10 cm^{-1}). For all tested samples, both $\nu_{E_{2g2}}$ and $\Delta\nu_{E_{2g2}}$ were found to increase linearly with $1/La$.

The analysis of the E_{2g1} Raman mode is more difficult, as its low frequency is close to the Rayleigh line, and required the use of a triplemonochromator spectrometer (Omars 89 from Dilor, according to the 45°-reflection macroscopic mode). The low frequency part of the spectra recorded for the A–BN, AC–BN and the

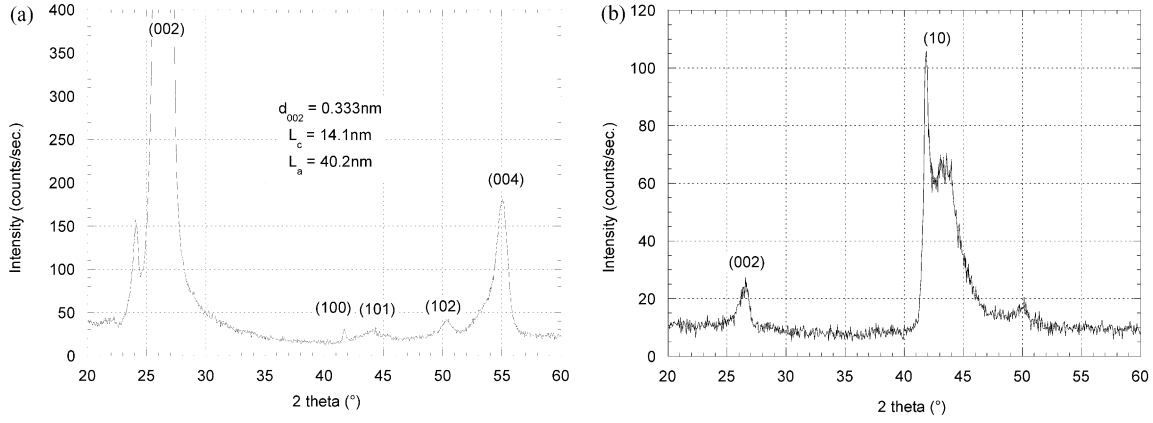

Fig. 5. XRD spectra of the Advanced Ceramics boron nitride (a) incidence normal to the substrate b) incidence parallel to the substrate.

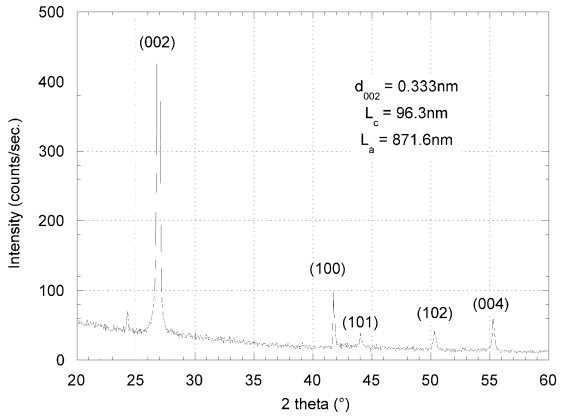

Fig. 6. XRD spectrum of the Aldrich boron nitride.

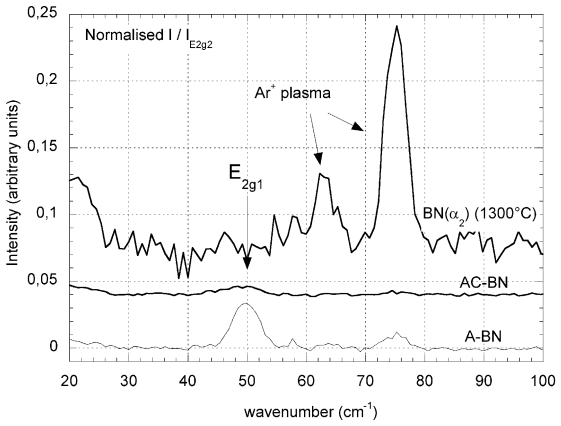

Fig. 8. Influence of the processing conditions on the E_{2g1} band.

BN(α_2) coating are shown in Fig. 8, after subtraction of the background and normalisation of the intensity with respect to that of the E_{2g2} mode. The sharp lines at 65 and 76 cm^{-1} are due to emissions of the Ar^+ plasma of the laser. The sharp band at 51 cm^{-1}, corresponding to the E_{2g1} mode, is due to the shear translational vibration of successive hexagonal planes in crystallised h-BN,[16] and so, denotes the marked tridimensional organisation of the A–BN. Whereas the similar E_{2g1} feature was observed for the AC-BN, though significantly weaker and broader, it was not observed for any of the coatings processed from the (BCl_3, NH_3, H_2) gas mixture. It is worthy of note that the spectra recorded from the presently studied BN coatings display particularly low signal/noise ratios (due their low thickness and to the macroscopic mode) and the presence of the E_{2g1} mode can not be therefore totally excluded. However, if a slight tridimensional (hexagonal) ordering is present in the high temperature CVD AC–BN material (as already suggested by XRD), it is likely less pronounced in the CVD–BN coatings studied here, the microstructure being mainly turbostratic. As a matter of fact, the coherence length *Lc* as determined by XRD does not exceed ≈10 nm for the CVD–BN coatings (Tables 3 and 4), whereas it is about 15 nm for the AC–BN and reaches 100 nm for A–BN.

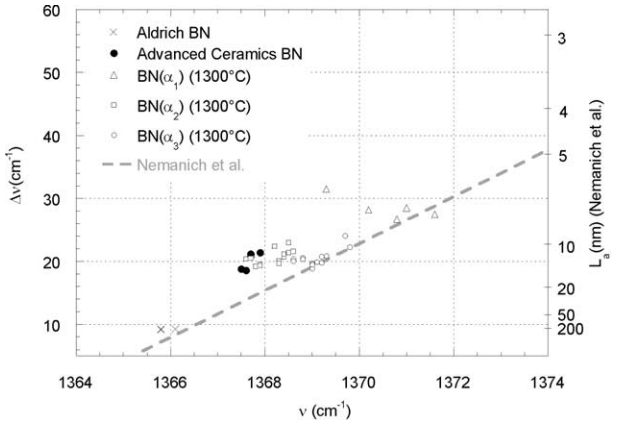

Fig. 7. Influence of the processing conditions on the E_{2g2} band features.

3.4. Scanning electron microscopy (SEM) observations

The fracture surface of the as-processed BN(α_1), BN(α_2) and BN(α_3) coatings show the same smooth appearance. Whereas the fracture surface of the BN(α_1) coating remains smooth after the post-deposition heat treatment, the BN(α_2) and BN(α_3) coatings show a strongly layered texture at a relatively low magnification (×13 000), suggesting an anisotropic microtexture of the boron nitride (Fig. 9).

3.5. TEM characterisation

The surface of the as-processed coatings shows the as-grown BN domains, characterised by the number of stacked layers, their lateral extension and their curvature. The lateral extension and the radius of curvature of the layers are both low for the BN(α_1) coating. The length of the layers (*La*) increases gradually with the α ratio (Fig. 10). While an ordering of all the BN coatings is generally observed after the heat treatment, the relation between the α ratio and the crystalline state of the boron nitride (in term of size of the layers) remains practically unchanged (Fig. 11). It is worthy of note that the TEM images shown in Fig. 11 were not obtained from the free surface of the coating, as in the as-deposited coating specimens, but from the core of the thicker coatings.

The BN(α_1) coating consists of crystallites having *La* values slightly longer than *Lc*. Some domains display a particularly high degree of crystallisation, leading to intense spots within the diffraction arcs on the SAD image (Fig. 11a). The small and distorted crystallites of the BN(α_1) deposit lead to an important nanoporosity. The relatively extended arcs of the SAD image confirm

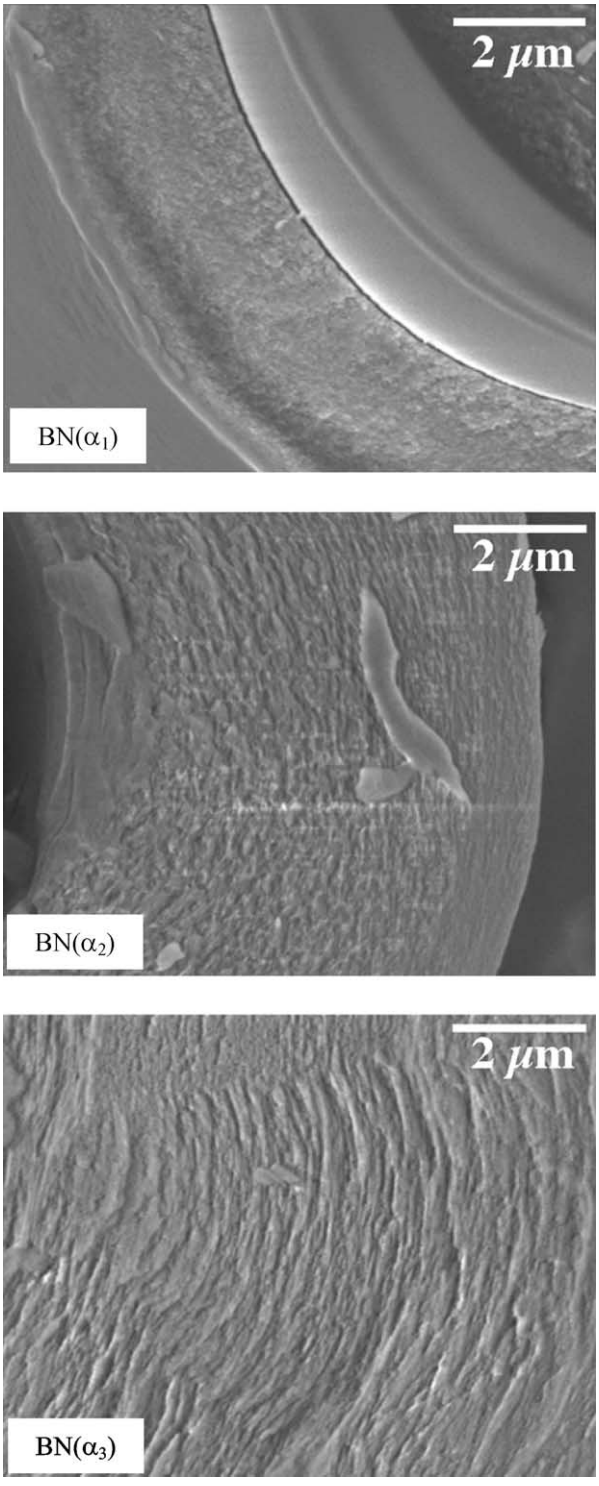

Fig. 9. SEM observations of the heat treated BN(α_1), BN(α_2) and BN(α_3) coatings.

the low anisotropy of the coating. The extension of the crystallites increases (*La* becomes significantly larger than *Lc*) and they organise parallel to the surface of the substrate when the α ratio increases, conferring an anisotropic texture to the coating, as confirmed by less extended arcs on the SAD images (Fig. 11b and c). Whereas poorly crystallised zones have been observed between the crystallites of the BN(α_2) coating (Fig. 11b), they are completely absent in the BN(α_3) coating (Fig. 11c).

The EELS spectra show sharp structures at the threshold (188 eV for B and 401 eV for N). These features are characteristic of hexagonal BN, as shown from the comparison with the spectrum of commercial h-BN (Fig. 12). In spite of some scattering of the data (Fig. 13), the EELS analyses tend to show an increase of the N/B ratio with α (respectively from N/B at. = 0.89–0.96 for α increasing of 0.6). This feature confirms the observations of some authors,[19,20] who have studied the influence of α on the composition of the coating. They have established that an excess of NH_3 with respect to BCl_3 in the gaseous phase is required to obtain quasi-stoichiometric boron nitride. The scattering of the data for the BN(α_3) coating makes difficult the analysis of the effect of the α ratio on the O/B ratio. Cholet et al.[10] have nevertheless observed that, because of the high reactivity of BCl_3 with oxygen, the B–O bonds can represent up to 30% of the total chemical bonds expected for boron (B–O, B–N, B–Cl) when BCl_3 is present in excess in the gaseous phase whereas there are only 10% of such chemical bonds for an excess of NH_3. The comparison of the N/B and O/B ratios obtained for the BN(α_1) and the BN(α_2) coatings seems indeed to show that the closer to stoichiometry the coating composition, the less sensitive to oxygen.

3.6. Discussion

In the same way that Jacques et al.[8] and Rebillat et al.,[9] who have established an evolution of the texture of the boron nitride with the processing parameters in the (BF_3, NH_3, Ar) system, Matsuda et al.[21] have observed, in the (BCl_3, NH_3, H_2) system and for a low processing pressure (2 kPa), a transition of the BN texture from isotropic to anisotropic at about 1300 °C. Matsuda et al.[21] have also showed that the temperature of the textural transition increases with the processing pressure. In the present work, the isotropic–anisotropic transition has been studied as a function of the α parameter, at given temperature and pressure.

Jacques et al.[8] have suggested that the geometry of the BF_3 and NH_3 molecules, which are respectively plane-trigonal and pyramidal-trigonal, might explain the differences in the texture of the coatings processed from an excess of BF_3 or NH_3 (the molecules being in excess in the gaseous phase, by absorbing preferentially on the substrate, would control the texture of the coating). Whereas BCl_3 and BF_3 have a similar geometry, the effect of the precursor gas ratio ($\alpha = Q_{NH3}/Q_{BX3}$ with X = Cl or F) on the anisotropy of the coating is reversed. An excess of BF_3 in the (BF_3, NH_3, Ar) system, leads to an anisotropic coating, versus an

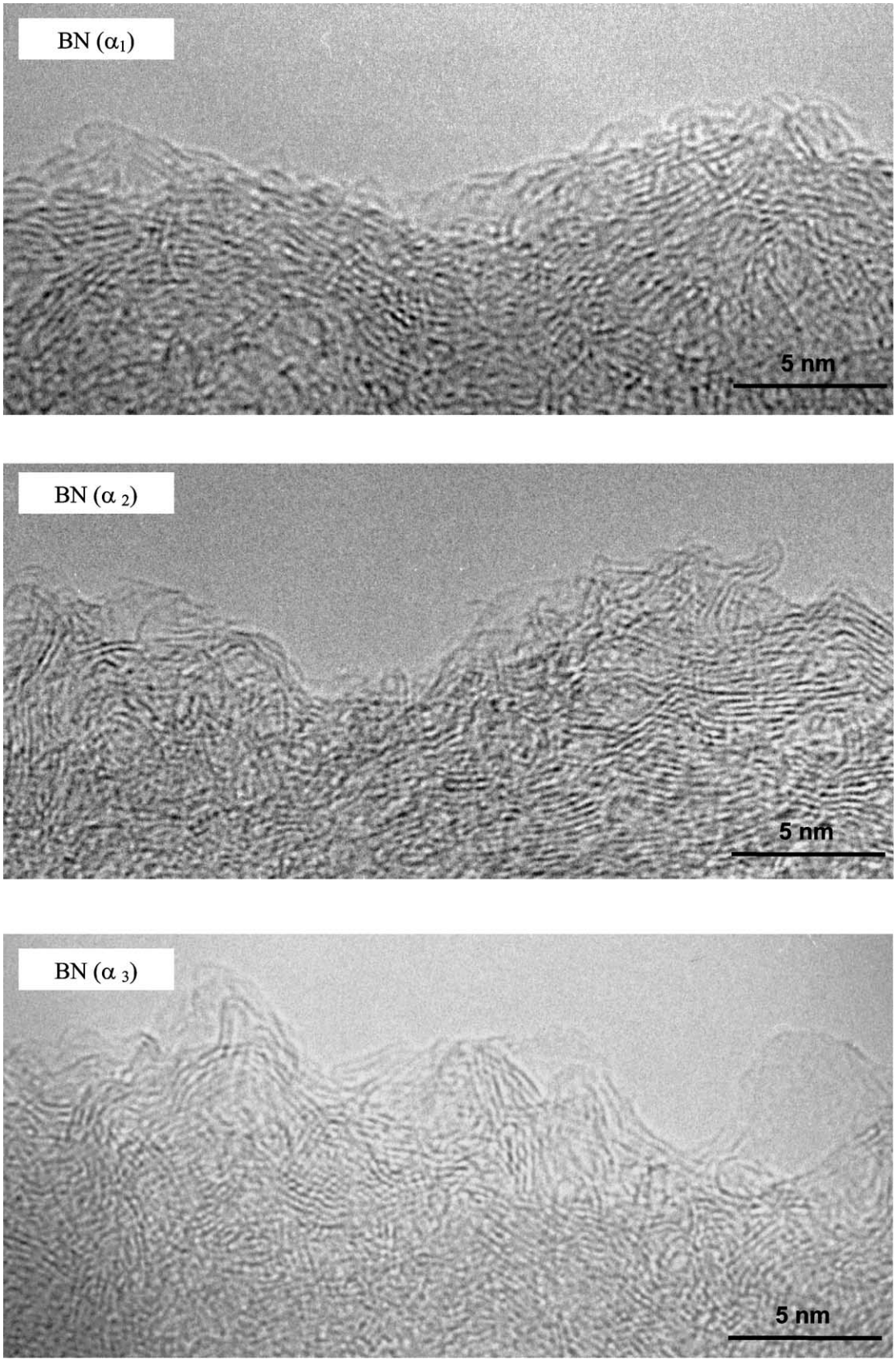

Fig. 10. HR TEM images of the surface of the as-processed BN(α_1), BN(α_2) and BN(α_3) coatings.

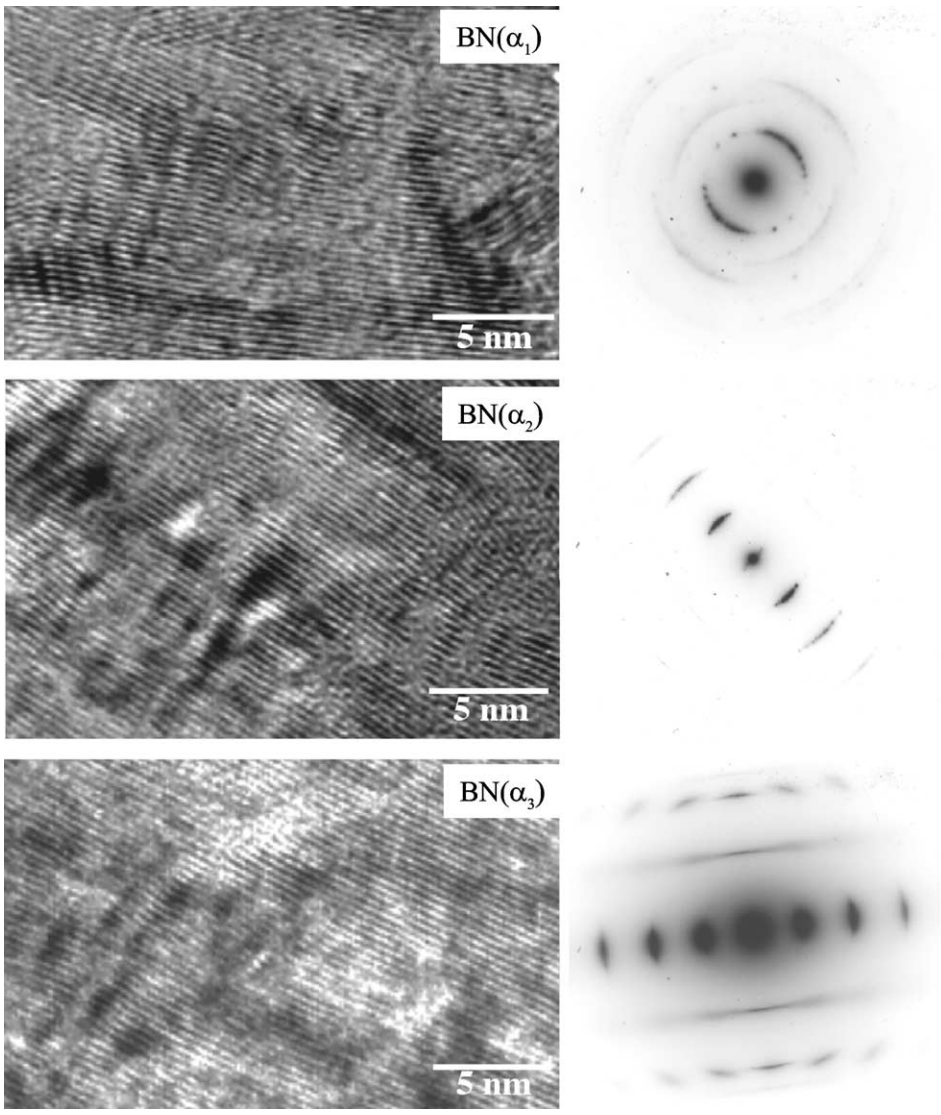

Fig. 11. HR TEM and SAD images of the heat treated BN deposits: (a) BN(α_1), (b) BN(α_2) and (c) BN(α_3) coatings.

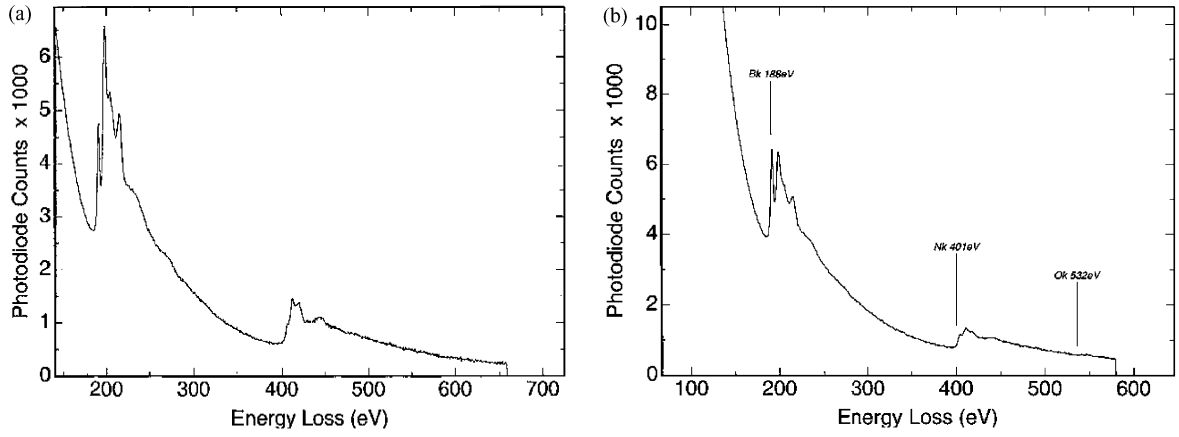

Fig. 12. EELS analyses of (a) a commercial h-BN and (b) the as-processed BN(α_1) coating.

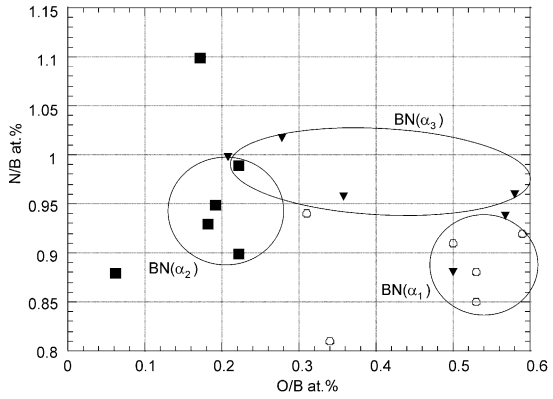

Fig. 13. EELS atomic concentration ratios of the as-processed BN(α_1), BN(α_2) and BN(α_3) coatings.

excess of NH_3 in the (BCl_3, NH_3, H_2) system. The evolution of the texture of the coating with the α parameter cannot therefore be only explained by the geometry of the molecules being in excess in the gaseous phase.

The CVD kinetic studies carried out by Prouhet[22] in the (BF_3, NH_3, Ar) system for different pressures, have shown the occurrence of two regimes: (i) a first low temperature domain where the kinetic of the deposition is controlled by the chemical reaction rates at the surface of the coating (chemical regime) and (ii) a second high temperature domain where the kinetic is rather controlled by the diffusion of the gas species through the boundary layer (mass transfer regime).

Jacques et al.,[8] who have studied conditions similar to those investigated by Prouhet[22] in term of α and β ratio, have directly correlated the change of the texture of the coating to the transition of the CVD rate controlling mechanism. According to Jacques et al., the deposition of anisotropic BN would correspond to a mass transfer regime, controlled by the diffusion of BCl_3. The deposition rate is indeed independent on the initial pressure of NH_3, for all the experimental conditions of pressure and temperature investigated.[22] According to these authors, such an apparent partial order value close to zero might be related to a major adsorption of NH_3 or derived specie such as for instance the Lewis adduct BF_3:NH_3. Tanji et al. have also suggested a similar interpretation for the (BCl_3, NH_3, H_2) system.[23]

Leparoux et al.[14] have shown that in the CVD conditions of the (BCl_3, NH_3, H_2) system, the kinetic was controlled by the combination of mass transfer and chemical reaction regimes, especially for low gas flows. A kinetic regime purely controlled by surface reactions was never observed for all the conditions investigated. The processing parameters used in the present study correspond to such low gas flow CVD conditions.

It is well known that, in the (BCl_3, NH_3, H_2) system, NH_3 partly reacts with HCl (a by-product of the CVD process) in the gas phase to form NH_4Cl. NH_3 may therefore rapidly be lacking in the gas phase if not present in sufficient excess with respect to BCl_3. The partial pressure of NH_3 might consequently control the kinetic of formation of BN at the surface of the sample, through a pure chemical reaction regime.

For the BN(α_1) coating, which is processed in the lowest NH_3 flow condition, the kinetic might therefore be governed by the role of both the NH_3 and BCl_3 species, i.e. the NH_3 partial pressure at the surface of the substrate, through a chemical reaction regime and the BCl_3 gas flow through a mass transfer regime. Conversely, for both the BN(α_2) and BN(α_3) coatings (which are processed with a higher NH_3 ratio), NH_3 might be in sufficient excess in the gas phase to result in kinetics mainly controlled by the BCl_3 gas flow only. The occurrence of an anisotropic BN coating from the (BCl_3, NH_3, H_2) system might therefore be associated to a mass transfer regime, i.e. a CVD mechanism where the diffusion of BCl_3 from the gas phase to the substrate is the rate controlling step.

4. Conclusion

The various processing conditions for the CVD of BN from the (BCl_3, NH_3, H_2) system have yield BN coatings displaying a wide range of microtextures (from isotropic to anisotropic), as widely illustrated by XRD, Raman microspectroscopy and TEM analyses. Specific CVD conditions associated with an appropriate post-deposition heat treatment were worked out to produce BN coatings with a microtexture suitable to be used in a CMC interphase. The crystallisation of the BN coatings was obtained by a heat treatment at a temperature well below that generally reported, owing to the introduction of controlled amounts of oxygen in the coatings. The crystallisation of the BN coating might occur according to a grain boundary diffusion mechanism, through the formation of boron and oxygen containing gaseous species. In addition to an appropriate post heat treatment, the best anisotropy of the BN coating is observed when NH_3 is present in excess with respect to BCl_3 in the gaseous phase. These processing conditions might be associated to a CVD mechanism where the kinetic is controlled by the diffusion of BCl_3 from the gas phase to the substrate.

Acknowledgements

This work was supported by DGA, through a grant given to S. Le Gallet and by Snecma. The authors would like to thank M. Alrivie, for the preparation of the TEM samples and F. Lamouroux from SPS in Le Haillan for valuable discussions.

References

1. Niedenzu, K. and Dawson, J. W., *Boron-Nitrogen Compounds*. Academic Press, New York, 1965.
2. *Handbook of Chemistry and Physics, 49th edn*. The Chemical Rubber Co, 1969.
3. Dugne, O., Prouhet, S., Guette, A., Naslain, R., Fourmeaux, R., Khin, Y., Sevely, J., Rocher, J. P. and Cotteret, J., Interface characterization by TEM, AES and SIMS in tough SiC (ex-PCS) fibre-SiC (CVI) matrix composites with a BN interphase. *J. Mater. Sci.*, 1993, **28**, 3409–3422.
4. Podobeda, L. G., Tsapuk, A. K. and Buravov, A. D., Oxidation of boron nitride under nonisothermal conditions. *Porshkovaya Metallurgiya*, 1976, **165**(9), 44–47.
5. Cofer, C. G. and Economy, J., Oxidative and hydrolitic stability of boron nitride. A new approach to improving the oxidation resistance of carbonaceous structures. *Carbon*, 1995, **33**(4), 389–395.
6. Rebillat, F., Guette, A. and Robin-Brosse, C., Chemical and mechanical alterations of SiC Nicalon fiber properties during CVD/CVI process of boron nitride. *Acta. Mater.*, 1999, **47**(5), 1685–1696.
7. Rebillat, F., Guette, A., Espitalier, L. and Naslain, R., Chemical and mechanical degradation of Hi-Nicalon and Hi-Nicalon S fibers under CVD/CVI BN processing condition. *Key Eng. Mater.*, 1999, **164–165**, 31–34.
8. Jacques, S., Vincent, H., Vincent, C., Lopez-Marure, A. and Bouix, J., Multilayered BN coatings processed by a continuous LPCVD treatment onto Hi-Nicalon fibers. *J. Solid State Chemistry*, 2001, **162**(2), 358–363.
9. Rebillat, F., Guette, A., Naslain, R. and Robin-Brosse, C., Highly ordered pyrolytic BN obtained by LPCVD. *J. Eur. Ceram. Soc.*, 1997, **17**, 1403–1414.
10. Cholet, V., Vandenbulcke, L., Rouan, J. P., Baillif, P. and Erre, R., Characterization of boron nitride films deposited from BCl_3–NH_3–H_2 mixtures in chemical vapour infiltration conditions. *J. Mater. Sci.*, 1994, **29**, 1417–1435.
11. Matsuda, T., Stability to moisture for chemically vapour-deposited boron nitride. *J. Mater. Sci.*, 1989, **24**, 2353–2358.
12. Lacrambe, G., *Fabrication et Graphitation du Nitrure de Bore Obtenu par Dépôt Chimique en Phase Vapeur à Basse Température*. PhD thesis, University of Bordeaux 1, No. 2232, 1988.
13. Rand, M. J. and Roberts, J. F., Preparation and properties of thin film boron nitride. *J. Electrochem. Soc.*, 1968, **115**(4), 423–429.
14. Leparoux, M., Vandenbulcke, L. and Clinard, C., Influence of isothermal chemical vapor deposition and chemical vapor infiltration conditions on the deposition kinetics and structure of boron nitride. *J. Am. Ceram. Soc.*, 1999, **82**(5), 1187–1195.
15. Thomas, J., Weston, N. E. and O'Connor, T. E., Turbostratic boron nitride, thermal transformation to ordered-layer-lattice boron nitride. *J. Am. Chem. Soc.*, 1963, **84**(24), 4619–4622.
16. Nemanich, R. J., Solin, S. A. and Martin, R. M., Light Scattering of boron nitride microcrystals. *Phys. Rev.*, 1981, **23**(1), 6348–6356.
17. Choi, Y. and Kang, S., Effect of B_2O_3 and hBN crystallinity on cBN synthesis. *J. Am. Ceram. Soc.*, 1993, **76**(10), 2525–2528.
18. Le Gallet, S., Rebillat, F., Guette, A. and Naslain, R., Oxidation resistance of CVD BN coatings: correlation with processing conditions and with precursor gas systems. In: *Proceedings of the 13th International Conference on Composite Materials, Beijing, 25–29 June 2001, CR-ROM* ed. Y. Zhang. ID1373, ISBN 7-900075-46-1.
19. Pippel, E., Woltersdorf, J., Dietrich, D., Stöckel, S., Weise, K. and Marx, G., CVD-coated boron nitride on continuous silicon carbide fibres: structure and nanocomposition. *J. Eur. Ceram. Soc.*, 2000, **20**, 1837–1844.
20. Huang, J., Pan, C. and Lii, D., Investigation of the BN films prepared by low pressure chemical vapor deposition. *Surface and Coatings Technology*, 1999, **122**, 166–175.
21. Matsuda, T., Nakae, H. and Hirai, T., Density and deposition rate of chemical vapour deposited boron nitride. *J. Mater. Sci.*, 1988, **23**, 509–514.
22. Prouhet, S., Langlais, F., Guette, A., Naslain, R. and Rey, J., On the kinetics of boron nitride CVD from BF_3–NH_3–Ar: 1. influence of temperature and total pressure on the kinetic control by mass transfer or chemical reactions. *Eur. J. Solid State Inorg. Chem.*, 1993, **30**, 953–969 and Prouhet, S., Vignoles, G., Langlais, F., Guette, A. and Naslain, R., 2. Influence of the precursor composition and chemical mechanisms, ibid. 971–989.
23. Tanji, H., Monden, K. and Ide, M., CVD mechanism of pyrolytic boron nitride. In: *Proceedings of the 10th International Conference on CVD, Pennington, 1987*, ed. G.W. Cullen (The Electrochem. Soc.). pp. 562–569.